

Safe Adaptive Control of Parabolic PDE-ODE Cascades*

Yun Jiang^a and Ji Wang^a

^aDepartment of Automation, Xiamen University, Xiamen 361005, China

Abstract

In this paper, we propose a safe adaptive boundary control strategy for a class of parabolic partial differential equation–ordinary differential equation (PDE–ODE) cascaded systems with parametric uncertainties in both the PDE and ODE subsystems. The proposed design is built upon an adaptive Control Barrier Function (aCBF) framework that incorporates high-relative-degree CBFs together with a batch least-squares identification (BaLSI)–based adaptive control that guarantees exact parameter identification in finite time. The proposed control law ensures that: (i) if the system output state initially lies within a prescribed safe set, safety is maintained for all time; otherwise, the output is driven back into the safe region within a preassigned finite time; and (ii) convergence to zero of all plant states is achieved. Numerical simulations are provided to demonstrate the effectiveness of the proposed approach.

Key words: Safe Adaptive Control; Parabolic PDE; Control Barrier Function; Backstepping.

1 Introduction

1.1 Boundary Control of Parabolic PDEs

Parabolic partial differential equations (PDEs) are widely employed to model dynamics in fluid flow, heat transfer, and chemical processes, with applications ranging from sea ice melting and freezing [11] to continuous steel casting [29] and lithium-ion battery systems [10], [34]. These applications naturally lead to significant control and estimation problems for parabolic PDEs. The backstepping approach [17] has been recognized as a powerful method for boundary stabilization/estimation of PDEs. The backstepping boundary control for parabolic PDEs was proposed in [22] and [21]. Since then, numerous advancements in boundary control and estimation of parabolic PDEs have been made over the past two decades, including [2], [3], [5], [6], [26], [28], [30], [37], [38], [39] and [45]. Besides the aforementioned studies on parabolic PDEs, there has been significant interest in parabolic PDE-ODE coupled systems, which arise in various physical contexts, including coupled electromagnetic, mechanical, and chemical reactions [35]. The backstepping stabilization of parabolic PDEs coupled with linear ODEs was initially explored in [13] for Dirichlet-type boundary interconnections, while results for Neumann boundary interconnections were later detailed in [33] and [35]. More recently, this framework has been extended to stabilize com-

plex chains where general LTI ODEs are interconnected with parabolic PDEs (featuring diffusion and counter-convection) through distributed coupling, as achieved by the n-step backstepping procedure in [49].

1.2 Safe Adaptive Control

The PDE control designs listed above mainly focus on stabilization and typically do not address safety requirements, i.e., guaranteeing that system outputs remain within prescribed safe sets during transients. However, safety is critical in applications such as autonomous vehicles, robotics, and UAVs. Control Barrier Functions (CBFs) provide a systematic framework for enforcing state constraints by ensuring the non-negativity of a barrier function [4]. Extensions to high relative-degree CBFs have been developed in [27,47,48], building on non-overshooting control concepts [14]. These ideas have enabled mean-square safety-critical stabilization [20] and prescribed-time safety guarantees [1]. Model uncertainties can invalidate safety guarantees derived from fully known models, motivating the recent interest in safe adaptive control. Most existing approaches are based on adaptive Control Lyapunov Functions (aCLFs) [15], with adaptive Control Barrier Functions (aCBFs) introduced in [36] to enforce safety under parametric uncertainties. Subsequent works reduced conservatism through data-driven estimation [24], hybrid adaptive laws [25], and certainty-equivalence-based designs [23].

* The material in this paper was not presented at any conference.

Email addresses: 34520241151611@stu.xmu.edu.cn (Yun Jiang), jiwang@xmu.edu.cn (Ji Wang).

Most existing results on safe adaptive control focus on systems governed by ODEs, while safe adaptive control for

PDE systems remains largely underexplored. For PDEs with fully known models, [12] introduced a CBF-based boundary control strategy for a parabolic Stefan system with actuator dynamics, and [42] studied safe output regulation of coupled hyperbolic PDEs. Recently, [42] proposed the first safe adaptive control framework for PDEs by developing an adaptive Control Barrier Function (aCBF) approach based on batch least-squares identification (BaLSI), which achieves finite-time parameter identification and was introduced in [8, 7] for nonlinear ODE, and extended to PDEs in [9, 41]. However, the method in [42] is limited to hyperbolic PDE–ODE cascades with parametric uncertainties. In contrast, this paper addresses a fundamentally different class of systems, namely parabolic PDE–ODE cascades, and develops a safe adaptive controller that guarantees both safety and convergence to zero of all states.

1.3 Main Contribution

- (1) Compared with existing adaptive boundary control for parabolic PDEs [32], [16], [31], [44], [19] and [18], the control design in this work further provides rigorous safety guarantees.
- (2) While [12] focuses on safe backstepping control for a Stefan model described by a parabolic PDE, this work addresses a broader class of problems by incorporating in-domain instabilities, parametric uncertainties, and more general safety constraints.
- (3) In contrast to the safe adaptive control for hyperbolic PDE–ODE cascades presented in [42], this paper considers parabolic PDE–ODE systems and accommodates more general safety constraints. To the best of our knowledge, this is the first result about safe adaptive control for parabolic PDEs.

1.4 Notation

- (1) The symbol \mathbb{Z}_+ denotes the set of all nonnegative integers.
- (2) We use the notation $L^2(0, 1)$ for the standard space of the equivalence class of square-integrable, measurable functions $f : (0, 1) \rightarrow \mathbb{R}$, with $\|f\|^2 := \int_0^1 f(x)^2 dx < +\infty$ for $f \in L^2(0, 1)$.
- (3) Let $u : \mathbb{R}_+ \times [0, 1] \rightarrow \mathbb{R}$ be given. We use the notation $u[t]$ to denote the profile of u at certain $t \geq 0$, i.e., $u[t](x) = u(x, t)$ for all $x \in [0, 1]$.
- (4) We use $p_x^{(i)}(x, t)$ to denote the i times partial derivatives with respect to x of $p(x, t)$. Similarly, $p_t^{(i)}(x, t)$ denotes i times partial derivatives with respect to t of $p(x, t)$. Define $\underline{z}_j := [z_1, z_2, \dots, z_j]^T$.

2 Problem Formulation

The considered plant is

$$\dot{Y}(t) = AY(t) + Bu(0, t), \quad (1)$$

$$u_t(x, t) = \varepsilon u_{xx}(x, t) + \lambda u(x, t), \quad (2)$$

$$u_x(0, t) = 0, \quad (3)$$

$$u(1, t) = U(t), \quad (4)$$

$\forall (x, t) \in [0, 1] \times [0, \infty)$. The function $U(t)$ is the control input to be designed and $u(x, t) \in \mathbb{R}$ is the state of the PDE, $Y(t) = [y_1(t), y_2(t), \dots, y_n(t)]^T \in \mathbb{R}^n$ is the state of the ODE. The column vector $B = [0, 0, \dots, b]^T$, where, without loss of generality, we consider $b > 0$. The matrix A is in the form of

$$A = \begin{pmatrix} a_{1,1} & 1 & 0 & 0 & \cdots & 0 \\ a_{2,1} & a_{2,2} & 1 & 0 & \cdots & 0 \\ \vdots & & & & & \\ a_{n-1,1} & a_{n-1,2} & a_{n-1,3} & a_{n-1,4} & \cdots & 1 \\ a_{n,1} & a_{n,2} & a_{n,3} & \cdots & a_{n,n-1} & a_{n,n} \end{pmatrix}, \quad (5)$$

where $a_{i,j}$ are arbitrary constants. This indicates that the Y-ODE is in the controllable form, which covers many practical models. The given safe barrier function h should satisfy Assumption 1. The positive constants b and λ are unknown parameters, which satisfy Assumption 2.

Assumption 1 *The time-varying function h is n times differentiable with respect to each of its arguments, i.e., y_1 as well as t , and satisfies that $\frac{\partial h(y_1, t)}{\partial y_1} \neq 0$, $\forall y_1 \in \{\ell \in \mathbb{R} | h(\ell, t) \geq 0\}$, $t \in [0, \infty)$ when h is positive at $t = 0$, or otherwise $\frac{\partial h(y_1, t)}{\partial y_1} \neq 0$, $\forall y_1 \in \mathbb{R}$, $t \in [0, \infty)$. Besides $|h(y_1(t), t)| < \infty \Rightarrow |y_1(t)| < \infty$ and $\lim_{t \rightarrow \infty} h(y_1(t), t) = 0 \Rightarrow \lim_{t \rightarrow \infty} y_1(t) = 0 \Rightarrow \lim_{t \rightarrow \infty} h_t^{(i)}(y_1(t), t) = 0$ for $i = 1, 2, \dots, n-1$.*

Assumption 2 *The bounds of the unknown parameters λ and b are known and arbitrary, i.e., $\underline{\lambda} \leq \lambda \leq \bar{\lambda}$, $0 < \underline{b} \leq b \leq \bar{b}$.*

3 Nominal Safe Control

3.1 Transformations for the distal ODE

Following [43], we propose the following two transformations to convert the ODE into a form of control barrier functions. The first transformation is

$$Z(t) = T_z Y(t), \quad (6)$$

where $Z(t) = [z_1(t), z_2(t), \dots, z_n(t)]^T$ and the matrix $T_z \in \mathbb{R}^{n \times n}$ are defined as

$$T_z = \begin{pmatrix} 1 & 0 & 0 & 0 & \cdots & 0 \\ \rho_{1,1} & 1 & 0 & 0 & \cdots & 0 \\ \rho_{2,1} & \rho_{2,2} & 1 & 0 & \cdots & 0 \\ \vdots & & & & & \\ \rho_{n-1,1} & \rho_{n-1,2} & \rho_{n-1,3} & \rho_{n-1,4} & \cdots & 1 \end{pmatrix}, \quad (7)$$

with the constants $\rho_{i,j}$ defined as

$$\rho_{1,1} = a_{1,1}, \quad (8)$$

$$\rho_{2,1} = a_{2,1} + \rho_{1,1}a_{1,1}, \quad \rho_{2,2} = a_{2,2} + \rho_{1,1}, \quad (9)$$

and for $i = 3, \dots, n$, as

$$\rho_{i,1} = a_{i,1} + \sum_{j=1}^{i-1} \rho_{i-1,j} a_{j,1}, \quad (10)$$

$$\rho_{i,i} = a_{i,i} + \rho_{i-1,i-1} + \sum_{j=1}^{i-1} \rho_{i-1,j} a_{j,i}, \quad i = 2, \dots, i-1, \quad (11)$$

$$\rho_{i,i} = a_{i,i} + \rho_{i-1,i-1}. \quad (12)$$

Applying the transformation (6), we now convert the Y-ODE in (1) into

$$\dot{Z}(t) = A_z Z(t) + Bu(0,t) + BK^T Y(t), \quad (13)$$

where

$$A_z = \begin{pmatrix} 0 & 1 & 0 & 0 & \cdots & 0 \\ 0 & 0 & 1 & 0 & \cdots & 0 \\ \vdots & & & & & \\ 0 & 0 & 0 & 0 & \cdots & 1 \\ 0 & 0 & 0 & 0 & \cdots & 0 \end{pmatrix}, \quad (14)$$

and

$$K^T = \frac{1}{b} [\rho_{n,1}, \rho_{n,2}, \dots, \rho_{n,n}]_{1 \times n}. \quad (15)$$

We apply the second transformation:

$$h_1(z_1(t), t) = h(y_1(t), t) + \sigma(t), \quad (16)$$

$$h_i(z_i(t), t) = \sum_{j=1}^{i-1} \frac{\partial h_{i-1}}{\partial z_j} z_{j+1} + \frac{\partial h_{i-1}}{\partial t} + \kappa_{i-1} h_{i-1}, \quad (17)$$

for $i = 2, 3, \dots, n$, with

$$\sigma(t) = \begin{cases} 0, & \text{if } h(y_1(0), 0) > 0, \\ \begin{cases} e^{\frac{1}{t_a}} (-h(y_1(0), 0) + \beta) e^{\frac{-1}{(t-t_a)^2}}, & t \in [0, t_a], \\ 0, & t \geq t_a, \end{cases} \\ \text{if } h(y_1(0), 0) \leq 0, \end{cases} \quad (18)$$

where t_a and β are arbitrarily positive design parameters. The function $\sigma(t)$, which is continuous and has continuous derivatives of all orders, is designed to address scenarios where the system states are in the unsafe region at the initial time $t = 0$. Specifically, when the initial state $y_1(0)$ falls outside the safe region, i.e., the condition $h(y_1(0), 0) \leq 0$, a new barrier function is created to guide the state return to the

safe region. The constant β indicates the distance from the safe barrier of the initial value of the new barrier function h_1 , and t_a is the upper bound of the time taken to return to the safe region.

According to Assumption 1, $h_1(z_1(t), t)$ is n times differentiable with respect to each of its arguments, i.e., z_1 and t . Noticing that $\dot{h}(y_1(t), t)$ denotes the full derivative with respect to t , whose calculation follows the chain rule, and $\frac{\partial h(y_1(t), t)}{\partial t}$ denotes the partial derivative with respect to t . Define

$$\frac{\partial h(y_1(t), t)}{\partial y_1(t)} = \vartheta(y_1(t), t) = \vartheta(z_1(t), t). \quad (19)$$

where $z_1(t) = y_1(t)$ according to (6) and (7). Considering the fact that $\frac{\partial h_n}{\partial z_n} = \frac{\partial h_{n-1}}{\partial z_{n-1}} = \dots = \frac{\partial h_1}{\partial z_1} = \frac{\partial h}{\partial y_1} = \vartheta$ that is obtained from (17), and applying (17) for $i = n$, we have

$$h_n(z_n(t), t) + \kappa_n h_n = b(\vartheta u(0, t) + f(z_n(t), t) + \vartheta K^T Y(t)), \quad (20)$$

where

$$f(z_n(t), t) = \frac{1}{b} \left(\sum_{j=1}^{n-1} \frac{\partial h_n}{\partial z_j} z_{j+1} + \frac{\partial h_n}{\partial t} + \kappa_n \left[\sum_{j=1}^{n-1} \frac{\partial h_{n-1}}{\partial z_j} z_{j+1} + \frac{\partial h_{n-1}}{\partial t} + \kappa_{n-1} h_{n-1} \right] \right). \quad (21)$$

Applying the second transformation (16) and (17), defining $H(t) = [h_1, \dots, h_n]^T$, we convert (13) into

$$\dot{H}(t) = A_h H(t) + B(\vartheta u(0, t) + f(z_n(t), t) + \vartheta K^T Y(t)), \quad (22)$$

where

$$A_h = \begin{pmatrix} -\kappa_1 & 1 & 0 & 0 & \cdots & 0 \\ 0 & -\kappa_2 & 1 & 0 & \cdots & 0 \\ \vdots & & & & & \\ 0 & 0 & 0 & 0 & \cdots & 1 \\ 0 & 0 & 0 & 0 & \cdots & -\kappa_n \end{pmatrix}. \quad (23)$$

3.2 PDE Backstepping Transformation

In order to remove the destabilizing term from the PDE and cancel the extra terms in (22), we introduce the following backstepping transformation:

$$w(x, t) = u(x, t) - \int_0^x k(x, y) u(y, t) dy - r(x) Y(t) - p(x, t), \quad (24)$$

with $k(x, y)$, $r(x)$, $p(x, t)$ satisfying

$$\varepsilon k_{xx}(x, y) = \varepsilon k_{yy}(x, y) + (\lambda + c)k(x, y), \quad (25)$$

$$k(x, x) = -\frac{\lambda + c}{2\varepsilon}x, \quad (26)$$

$$k_y(x, 0) = -r(x)\frac{B}{\varepsilon}, \quad (27)$$

$$\varepsilon \ddot{r}(x) = r(x)(A + cI), \quad (28)$$

$$r(0) = -K^T, \quad \dot{r}(0) = 0, \quad (29)$$

$$p_t(x, t) = \varepsilon p_{xx}(x, t) - cp(x, t), \quad (30)$$

$$p_x(0, t) = 0, \quad p(0, t) = -\frac{1}{\vartheta(z_1(t), t)}f(z_n(t), t), \quad (31)$$

where c is a positive constant, and $\vartheta(z_1(t), t)$ is nonzero according to Assumption 1. The solutions of (25)–(31) are given in Appendix A.

With (24), the original system (2)–(4) with (22) is converted into the following system

$$\dot{H}(t) = A_h H(t) + B\vartheta w(0, t), \quad (32)$$

$$w_t(x, t) = \varepsilon w_{xx}(x, t) - cw(x, t), \quad (33)$$

$$w_x(0, t) = 0, \quad (34)$$

$$w(1, t) = \delta(t), \quad (35)$$

by choosing the control input as

$$U(t) = \int_0^1 k(1, y)u(y, t)dy + r(1)Y(t) + \delta(t) + p(1, t), \quad (36)$$

where $\delta(t)$ is designed as the following form

$$\delta(t) = \text{sign}(\vartheta)M e^{-ct}, \quad (37)$$

with $M > 0$ is a design parameter to be determined later.

3.3 Selection of safe design parameters

The design parameters κ_i , $i = 1, 2, \dots, n$ are selected to satisfy

$$\kappa_i > \max\{0, \dot{\kappa}_i\}, \quad i = 1, 2, \dots, n-1, \quad (38)$$

$$\kappa_n \leq c, \quad (39)$$

where

$$\dot{\kappa}_i = \frac{-1}{h_i(\underline{z}_i(0), 0)} \left[\sum_{j=1}^i \frac{\partial h_i}{\partial z_j} z_{j+1}(0) + \frac{\partial h_i}{\partial t} \right]. \quad (40)$$

The gain condition (38) ensures the following lemma.

Lemma 1 *With the design parameters κ_i , $i = 1, 2, \dots, n-1$ satisfying (38), the high-relative-degree ODE CBFs is initialized positive, i.e., $h_i(\underline{z}_i(0), 0) > 0$ for $i = 1, 2, \dots, n$.*

Proof. According to (16) and (18), we know $h_1(z_1(0), 0) > 0$. Recalling (17), we have $h_i(\underline{z}_i(0), 0) = \sum_{j=1}^{i-1} \frac{\partial h_{i-1}}{\partial z_j} z_{j+1}(0) + \frac{\partial h_{i-1}}{\partial t} + \kappa_{i-1} h_{i-1}(\underline{z}_{i-1}(0), 0)$ for $i = 2, 3, \dots, n$. Choosing κ_i to satisfy (38) and (40), we can obtain that $h_i(\underline{z}_i(0), 0) > 0$ for $i = 2, 3, \dots, n$. The proof is complete. \square

3.4 Result of the nominal safe control

Theorem 1 *For initial condition $u[0] \in L^2(0, 1)$ and $Y(0) \in \mathbb{R}^n$, if design parameters κ_i , $i = 1, 2, \dots, n-1$ satisfy (38) and κ_n satisfies $\kappa_n \leq c$, the closed-loop system consisting of the plant (1)–(4) and the control law (36) have the following properties:*

(1) *All states are convergent to zero, i.e.,*

$$\lim_{t \rightarrow \infty} (\|u_x(\cdot, t)\|^2 + \|u(\cdot, t)\|^2 + |Y(t)|^2) = 0.$$

(2) *Safety is ensured in the sense that if $h(y_1(0), 0) > 0$, then $h(y_1(t), t) \geq 0$ for all $t \geq 0$; if $h(y_1(0), 0) \leq 0$, then there exists a finite time $t_a > 0$ such that $h(y_1(t), t) \geq 0$ for all $t \geq t_a$, where t_a can be arbitrarily assigned by users.*

Proof. (1) We show that the convergence to zero of all states in property 1 is achieved by Lyapunov analysis. Defining the following transformation:

$$w(x, t) = v(x, t) + \delta(t). \quad (41)$$

Considering (37), we have

$$\dot{H}(t) = A_h H(t) + B\vartheta v(0, t) + B\vartheta \delta(t), \quad (42)$$

$$v_t(x, t) = \varepsilon v_{xx}(x, t) - cv(x, t), \quad (43)$$

$$v_x(0, t) = 0, \quad (44)$$

$$v(1, t) = 0. \quad (45)$$

Define the Lyapunov function

$$V(t) = H(t)^T P H(t) + \frac{1}{2} \int_0^1 v(x, t)^2 dx + \frac{a_1}{2} \int_0^1 v_x(x, t)^2 dx + \frac{a_2}{2} \delta(t)^2, \quad (46)$$

where the positive definite matrix $P = P^T$ is the solution of the Lyapunov equation $A_h^T P + P A_h = -Q$ for some $Q = Q^T > 0$, and where the positive analysis parameters a_1 and a_2 are to be determined later. Defining

$$\Xi(t) = |H(t)|^2 + \|v(\cdot, t)\|^2 + \|v_x(\cdot, t)\|^2 + \delta(t)^2, \quad (47)$$

we have

$$\xi_1 \Xi(t) \leq V(t) \leq \xi_2 \Xi(t), \quad (48)$$

for some positive ξ_1 and ξ_2 . Taking the time derivative of $V(t)$, applying Young's inequality and Cauchy-Schwarz inequality, we have

$$\begin{aligned}
\dot{V}(t) &= -H(t)^T Q H(t) + 2H(t)^T P B \vartheta v(0, t) \\
&\quad + 2H(t)^T P B \vartheta \delta(t) + \int_0^1 v(x, t) v_t(x, t) dx \\
&\quad + a_1 \int_0^1 v_x(x, t) v_{x,t}(x, t) dx - a_2 c \delta(t)^2 \\
&\leq -\lambda_{\min}(Q) H(t)^2 + \frac{\lambda_{\min}(Q)}{3} H(t)^2 \\
&\quad + \frac{3|PB|^2}{\lambda_{\min}(Q)} \bar{\vartheta}^2 v(0, t)^2 - a_2 c \delta(t)^2 \\
&\quad + \frac{\lambda_{\min}(Q)}{3} H(t)^2 + \frac{3|PB|^2}{\lambda_{\min}(Q)} \vartheta^2 \delta(t)^2 \\
&\quad - \varepsilon \int_0^1 v_x(x, t)^2 dx - c \int_0^1 v(x, t)^2 dx \\
&\quad - a_1 \varepsilon \int_0^1 v_{xx}(x, t)^2 dx - a_1 c \int_0^1 v_x(x, t)^2 dx \\
&\leq -\frac{\lambda_{\min}(Q)}{3} H(t)^2 - c \int_0^1 v(x, t)^2 dx \\
&\quad - \left(\varepsilon + a_1 c - \frac{3|PB|^2 \bar{\vartheta}^2}{\lambda_{\min}(Q)} \right) \int_0^1 v_x(x, t)^2 dx \\
&\quad - \left(a_2 c - \frac{3|PB|^2 \bar{\vartheta}^2}{\lambda_{\min}(Q)} \right) \delta(t)^2,
\end{aligned}$$

where $\bar{\vartheta}$ is the upper bound of $\vartheta = \frac{\partial h}{\partial y_1}$ that is bounded according to Assumption 1 that means that h is n times differentiable with respect to y_1 . Choosing a_1 and a_2 large enough to satisfy

$$a_1 > \max \left\{ \frac{3|PB|^2 \bar{\vartheta}^2}{c \lambda_{\min}(Q)} - \frac{\varepsilon}{c}, 0 \right\}, \quad (49)$$

$$a_2 > \frac{3|PB|^2 \bar{\vartheta}^2}{c \lambda_{\min}(Q)}, \quad (50)$$

we then obtain that

$$\dot{V}(t) \leq -\gamma V(t), \quad (51)$$

where

$$\begin{aligned}
\gamma &= \frac{1}{\xi_2} \min \left\{ \frac{\lambda_{\min}(Q)}{3}, \varepsilon + a_1 c - \frac{3|PB|^2 \bar{\vartheta}^2}{\lambda_{\min}(Q)}, \right. \\
&\quad \left. c, a_2 c - \frac{3|PB|^2 \bar{\vartheta}^2}{\lambda_{\min}(Q)} \right\}.
\end{aligned} \quad (52)$$

Recalling (48), it follows that

$$\Xi(t) \leq \frac{\xi_2}{\xi_1} \Xi(0) e^{-\gamma t}. \quad (53)$$

Next, we show the convergence to zero of the original states from the target system's stability obtained from (53). From Assumption 1, (16) and the convergence to zero of $|H(t)|$ obtained from (53), we have $y_1(t) = z_1(t)$ converge to zero. Then recalling (17) for $i = 2$, together with the convergence to zero of $h_1(t)$ and $h_2(t)$ as well as Assumption 1, we obtain that $z_2(t)$ converge to zero. Through the recursive process, we obtain that $|Z(t)|$ is convergent to zero. According to the transformation defined in (6), the convergence of $|Y(t)|$ is obtained. The inverse of (24) is obtained as

$$\begin{aligned}
u(x, t) &= w(x, t) - \int_0^x \bar{k}(x, y) w(y, t) dy \\
&\quad - \bar{r}(x) Y(t) - \bar{p}(x, t),
\end{aligned} \quad (54a)$$

where the solutions of $\bar{k}(x, y)$, $\bar{r}(x)$ and $\bar{p}(x, t)$ can be obtained similarly to those in the transformation (24). Using the convergence to zero of $\|w(\cdot, t)\|$, $\|w_x(\cdot, t)\|$ obtained from the convergence of $\|v(\cdot, t)\|$, $\|v_x(\cdot, t)\|$, $\delta(t)$, $|Y(t)|$, and $\|\bar{p}(\cdot, t)\|$, $\|\bar{p}_x(\cdot, t)\|$, we obtain the convergence of $\|u(\cdot, t)\|$, $\|u_x(\cdot, t)\|$ via (54a). The property 1 is obtained.

(2) According to (23), (32), we have

$$\begin{aligned}
h_n(\underline{z}_n(t), t) &= e^{-\kappa_n t} h_n(\underline{z}_n(0), 0) \\
&\quad + e^{-\kappa_n t} b \int_0^t e^{\kappa_n \tau} \vartheta w(0, \tau) d\tau
\end{aligned} \quad (55)$$

$$\begin{aligned}
&= e^{-\kappa_n t} (h_n(\underline{z}_n(0), 0) \\
&\quad + b \int_0^t e^{\kappa_n \tau} \vartheta w(0, \tau) d\tau).
\end{aligned} \quad (56)$$

It is obvious that $h_n(\underline{z}_n(t), t) > 0$ if $h_n(\underline{z}_n(0), 0) + b \int_0^t e^{\kappa_n \tau} \vartheta w(0, \tau) d\tau > 0$ for all $t \geq 0$. Recalling (32)–(35), the solution $w(x, t)$ is obtained as

$$\begin{aligned}
w(x, t) &= \delta(t) + \sum_{j=0}^{\infty} \cos\left(\left(\frac{\pi}{2} + j\pi\right)x\right) \left[e^{-(\varepsilon(\frac{\pi}{2} + j\pi)^2 + c)t} \theta_j - \right. \\
&\quad \left. \frac{2(-1)^j}{\frac{\pi}{2} + j\pi} \int_0^t e^{-(\varepsilon(\frac{\pi}{2} + j\pi)^2 + c)(t-\tau)} (c\delta(\tau) + \dot{\delta}(\tau)) d\tau \right], \quad (57)
\end{aligned}$$

where

$$\theta_j = 2 \int_0^1 [w(x, 0) - \delta(0)] \cos\left(\left(\frac{\pi}{2} + j\pi\right)x\right) dx.$$

The detailed process for solving $w(x, t)$ is presented in the Appendix B. Considering (57), choosing $\kappa_n \leq c$, and recalling (37), we have

$$\begin{aligned}
h_n(\underline{z}_n(0), 0) &+ b \int_0^t e^{\kappa_n \tau} \vartheta w(0, \tau) d\tau \\
&= 2b \int_0^t e^{(\kappa_n - c)\tau} \left(\vartheta \sum_{j=0}^{+\infty} e^{-\varepsilon(\frac{\pi}{2} + j\pi)^2 \tau} \theta_j \right) d\tau \\
&\quad + h_n(\underline{z}_n(0), 0) + bM \int_0^t e^{(\kappa_n - c)\tau} \vartheta \left[\text{sign}(\vartheta) \right]
\end{aligned}$$

$$-2\text{sign}(\vartheta(y_1(0)), 0) \sum_{j=0}^{+\infty} e^{-\varepsilon(\frac{\pi}{2}+j\pi)^2\tau} \frac{(-1)^j}{\frac{\pi}{2}+j\pi} \Big] d\tau, \quad (58)$$

where

$$\dot{\theta}_j = \int_0^1 w(x, 0) \cos\left(\frac{\pi}{2} + j\pi\right) x dx. \quad (59)$$

Obviously, there exists a finite time $t_M > 0$ such that

$$2b \int_0^t e^{(\kappa_n-c)\tau} \left(\vartheta \sum_{j=0}^{+\infty} e^{-\varepsilon(\frac{\pi}{2}+j\pi)^2\tau} \dot{\theta}_j \right) d\tau + h_n(\underline{z}_n(0), 0) \quad (60)$$

is non-negative for all $t \in [0, t_M]$ since $h_n(\underline{z}_n(0), 0) > 0$. Considering the fact that

$$\begin{aligned} & \int_0^t e^{(\kappa_n-c)\tau} \vartheta \left[\text{sign}(\vartheta) \right. \\ & \left. - 2\text{sign}(\vartheta(y_1(0), 0)) \sum_{j=0}^{+\infty} e^{-\varepsilon(\frac{\pi}{2}+j\pi)^2\tau} \frac{(-1)^j}{\frac{\pi}{2}+j\pi} \right] d\tau \geq 0, \end{aligned} \quad (61)$$

whose proof is presented in the Appendix C, we thus obtain $h_n(\underline{z}_n(t), t) > 0$ for all $t \in [0, t_M]$. By choosing M to satisfy

$$M > \frac{\sup_{t \geq t_M} \left| 2 \sum_{j=0}^{+\infty} e^{-\varepsilon(\frac{\pi}{2}+j\pi)^2 t} \dot{\theta}_j \right|}{1 - 2 \sum_{j=0}^{+\infty} e^{-\varepsilon(\frac{\pi}{2}+j\pi)^2 t_M} \frac{(-1)^j}{\frac{\pi}{2}+j\pi}}, \quad (62)$$

where the proof of the convergence of the series in (62) is given in Appendix E, we obtain that $h_n(\underline{z}_n(t), t) > 0$ for all $t \geq 0$, whose proof is presented at Appendix D.

According to (22), (23) and the parameters κ_i , $i = 1, 2, \dots, n-1$ satisfying (38) and (40), we obtain that $h_1(z_1(t), t) > 0$ for all $t \geq 0$. Now we show safety in the following two cases:

Case 1. When $h(y_1(0), 0) > 0$, it is obtained from (18) that $\sigma(t) = 0$. Recalling (16), we have $h_1(z_1(t), t) = h(y_1(t), t) > 0$ for all $t \geq 0$;

Case 2. When $h(y_1(0), 0) \leq 0$, it is obtained from (18) that $\sigma(t) = 0$ for $t \geq t_a$. According to (16), we know $h_1(z_1(t), t) = h(y_1(t), t) > 0$ for $t \geq t_a$.

The proof of this theorem is complete. \square

4 Safe adaptive control design

Defining $\theta = [\lambda, b]^T$, replacing the unknown parameters λ, b in the nominal controller (36) with the parameter estimates, we have

$$U_d(t) := U(t, \hat{\theta}(t_i)), \quad t \in [t_i, t_{i+1}), \quad (63)$$

where

$$\hat{\theta} = [\hat{\lambda}, \hat{b}]^T, \quad (64)$$

is an estimation generated by a triggered batch least-squares identifier that will be defined later, and where the sequence of time instants t_i is defined as

$$t_{i+1} = t_i + T, \quad (65)$$

with T as a free positive design parameter.

4.1 Batch least-squares identifier

According to (1) and (2), similar to [40], we obtain for $\tau > 0$ and $\bar{n} = 1, 2, \dots$ that

$$\begin{aligned} \frac{d}{d\tau} \int_0^1 \sin(x\pi\bar{n}) u(x, \tau) dx &= -\varepsilon(\pi\bar{n})(-1)^{\bar{n}} u(1, \tau) \\ &+ \varepsilon(\pi\bar{n}) u(0, \tau) - \varepsilon(\pi\bar{n})^2 \int_0^1 \sin(x\pi\bar{n}) u(x, \tau) dx \\ &+ \lambda \int_0^1 \sin(x\pi\bar{n}) u(x, \tau) dx, \end{aligned} \quad (66)$$

$$\frac{d}{d\tau} y_n(\tau) = \sum_{i=1}^n a_{ni} y_i(\tau) + b u(0, \tau). \quad (67)$$

Define the instant μ_{i+1} as

$$\mu_{i+1} = \min\{t_j : j \in \{0, \dots, i\}, t_j \geq t_{i+1} - \bar{N}T\}, \quad (68)$$

for $i \in \mathbb{Z}^+$, where the positive integer $\bar{N} \geq 1$ is a free design parameter. Integrating (66) and (67) from μ_{i+1} to t , we obtain

$$p_{\bar{n}}(t, \mu_{i+1}) = \lambda g_{\bar{n}}(t, \mu_{i+1}), \quad p_b(t, \mu_{i+1}) = b q_b(t, \mu_{i+1}), \quad (69)$$

where $p_{\bar{n}}$, $g_{\bar{n}}$, p_b and q_b are

$$\begin{aligned} p_{\bar{n}}(t, \mu_{i+1}) &= \int_0^1 \sin(x\pi\bar{n}) u(x, t) dx \\ &+ \varepsilon\pi\bar{n}(-1)^{\bar{n}} \int_{\mu_{i+1}}^t u(1, \tau) d\tau - \varepsilon\pi\bar{n} \int_{\mu_{i+1}}^t u(0, \tau) d\tau \\ &+ \varepsilon(\pi\bar{n})^2 \int_{\mu_{i+1}}^t \int_0^1 \sin(x\pi\bar{n}) u(x, \tau) dx d\tau \\ &- \int_0^1 \sin(x\pi\bar{n}) u(x, \mu_{i+1}) dx, \end{aligned} \quad (70)$$

$$g_{\bar{n}}(t, \mu_{i+1}) = \int_{\mu_{i+1}}^t \int_0^1 \sin(x\pi\bar{n}) u(x, \tau) dx d\tau, \quad (71)$$

for $\bar{n} = 1, 2, \dots$ and

$$p_b(t, \mu_{i+1}) = y_n(t) - y_n(\mu_{i+1}) - \int_{\mu_{i+1}}^t \sum_{i=1}^n a_{ni} y_i(\tau) d\tau, \quad (72)$$

$$q_b(t, \mu_{i+1}) = \int_{\mu_{i+1}}^t u(0, \tau) d\tau. \quad (73)$$

Define a function $h_{i,\bar{n}} : \mathbb{R}^3 \rightarrow \mathbb{R}_+$ by the formula

$$h_{i,\bar{n}}(\ell) = \int_{\mu_{i+1}}^{t_{i+1}} \left[(p_{\bar{n}}(t, \mu_{i+1}) - \ell_1 g_{\bar{n}}(t, \mu_{i+1}))^2 + (p_b(t, \mu_{i+1}) - \ell_2 q_b(t, \mu_{i+1}))^2 \right] dt, \quad (74)$$

for $i \in \mathbb{Z}^+$, where $\ell = [\ell_1, \ell_2]^T$. According to (69), the function $h_{i,\bar{n}}(\ell)$ has a global minimum $h_{i,\bar{n}}(\theta) = 0$. We get from the Fermat's theorem (vanishing gradient at extrema), that is, differentiating the functions $h_{i,\bar{n}}(\ell)$ defined by (74) with respect to ℓ_1, ℓ_2 respectively and making the derivatives at the position of the global minimum $[\ell_1, \ell_2] = [\lambda, b]$ as zero, that the following matrix equation holds for every $i \in \mathbb{Z}^+$ and $\bar{n} = 1, 2, \dots$:

$$Z_{\bar{n}}(\mu_{i+1}, t_{i+1}) = G_{\bar{n}}(\mu_{i+1}, t_{i+1})\theta, \quad (75)$$

where $\theta = [\lambda, b]^T$ is a column vector of the unknown parameters, and where

$$Z_{\bar{n}} = [H_{\bar{n},1}, H_2]^T, \quad G_{\bar{n}} = \begin{bmatrix} Q_{\bar{n},1} & 0 \\ 0 & Q_2 \end{bmatrix}, \quad (76)$$

with $H_{\bar{n},1}, H_2, Q_{\bar{n},1}$ and Q_2 defined as

$$H_{\bar{n},1}(\mu_{i+1}, t_{i+1}) = \int_{\mu_{i+1}}^{t_{i+1}} p_{\bar{n}}(t, \mu_{i+1}) g_{\bar{n}}(t, \mu_{i+1}) dt, \quad (77)$$

$$H_2(\mu_{i+1}, t_{i+1}) = \int_{\mu_{i+1}}^{t_{i+1}} p_b(t, \mu_{i+1}) q_b(t, \mu_{i+1}) dt, \quad (78)$$

$$Q_{\bar{n},1}(\mu_{i+1}, t_{i+1}) = \int_{\mu_{i+1}}^{t_{i+1}} g_{\bar{n}}(t, \mu_{i+1})^2 dt, \quad (79)$$

$$Q_2(\mu_{i+1}, t_{i+1}) = \int_{\mu_{i+1}}^{t_{i+1}} q_b(t, \mu_{i+1})^2 dt. \quad (80)$$

The parameter estimator (update law) is defined as

$$\begin{aligned} \hat{\theta}(t_{i+1}) &= \arg \min \{ |\ell - \hat{\theta}(t_i)|^2 : \ell \in \Theta, \\ Z_{\bar{n}}(\mu_{i+1}, t_{i+1}) &= G_{\bar{n}}(\mu_{i+1}, t_{i+1})\ell, \bar{n} = 1, 2, \dots \}, \end{aligned} \quad (81)$$

where

$$\Theta = \{ \ell \in \mathbb{R}^2 : \underline{\lambda} \leq \lambda \leq \bar{\lambda}, 0 < \underline{b} \leq b \leq \bar{b} \}. \quad (82)$$

4.2 Safe Adaptive Controller

Defining $e(t) = U(t) - U_d(t)$ as the control input error between (63) and (36), through the same process in Sec. 3.2, the target system is rewritten as

$$\dot{H}(t) = A_h H(t) + B \vartheta w(0, t), \quad (83)$$

$$w_t(x, t) = \varepsilon w_{xx}(x, t) - cw(x, t), \quad (84)$$

$$w_x(0, t) = 0, \quad (85)$$

$$w(1, t) = \delta(t) + e(t), \quad (86)$$

where, as shown in Appendix B, $w(x, t)$ is solved as

$$\begin{aligned} w(x, t) &= \delta(t) + e(t) + \sum_{j=0}^{\infty} \left[e^{-(\varepsilon(\frac{\pi}{2} + j\pi)^2 + c)t} \theta_j - \right. \\ &\quad \left. \frac{2(-1)^j}{\frac{\pi}{2} + j\pi} \int_0^t e^{-(\varepsilon(\frac{\pi}{2} + j\pi)^2 + c)(t-\tau)} (c\delta(\tau) \right. \\ &\quad \left. + ce(\tau) + \dot{\delta}(\tau) + \dot{e}(\tau)) d\tau \right] \cos((\frac{\pi}{2} + j\pi)x). \end{aligned} \quad (87)$$

Through the same process applied in (58), we obtain that

$$\begin{aligned} h_n(\underline{z}_n(0), 0) &+ b \int_0^t e^{\kappa_n \tau} \vartheta w(0, \tau) d\tau \\ &= h_n(\underline{z}_n(0), 0) + 2b \int_0^t e^{(\kappa_n - c)\tau} \vartheta \left(\sum_{j=0}^{+\infty} e^{-\varepsilon(\frac{\pi}{2} + j\pi)^2 \tau} \dot{\theta}_j \right. \\ &\quad \left. + \sum_{j=0}^{+\infty} \frac{(-1)^j}{\frac{\pi}{2} + j\pi} e^{-\varepsilon(\frac{\pi}{2} + j\pi)^2 \tau} \left(e(0) \right. \right. \\ &\quad \left. \left. + \int_0^{\tau} \varepsilon(\frac{\pi}{2} + c)^2 e^{(\varepsilon(\frac{\pi}{2} + j\pi)^2 + c)\eta} e(\eta) d\eta \right) \right) d\tau \\ &\quad + bM \int_0^t e^{(\kappa_n - c)\tau} \vartheta \left[\text{sign}(\vartheta) \right. \\ &\quad \left. - 2 \text{sign}(\vartheta(y_1(0), 0)) \sum_{j=0}^{+\infty} e^{-\varepsilon(\frac{\pi}{2} + j\pi)^2 \tau} \frac{(-1)^j}{\frac{\pi}{2} + j\pi} \right] d\tau \end{aligned} \quad (88)$$

which is different with (58) due to the presence of the control input error $e(t)$. Considering $h_n(\underline{z}_n(0), 0) > 0$, we know t_M generated by the following triggering condition

$$\begin{aligned} t_M &= \inf \left\{ t \geq 0 : h_n(\underline{z}_n(0), 0) \right. \\ &\quad \left. + \max_{\underline{\lambda} \leq \lambda \leq \bar{\lambda}, 0 < \underline{b} \leq b \leq \bar{b}} 2b \int_0^t e^{(\kappa_n - c)\tau} \vartheta \left(\sum_{j=0}^{+\infty} e^{-\varepsilon(\frac{\pi}{2} + j\pi)^2 \tau} \dot{\theta}_j \right. \right. \\ &\quad \left. \left. + \sum_{j=0}^{+\infty} \frac{(-1)^j}{\frac{\pi}{2} + j\pi} e^{-\varepsilon(\frac{\pi}{2} + j\pi)^2 \tau} \left(e(0) \right. \right. \right. \\ &\quad \left. \left. \left. + \int_0^{\tau} \varepsilon(\frac{\pi}{2} + c)^2 e^{(\varepsilon(\frac{\pi}{2} + j\pi)^2 + c)\eta} e(\eta) d\eta \right) \right) d\tau \leq 0 \right\}, \end{aligned} \quad (89)$$

is larger than zero. Meanwhile, considering that $w(x, 0)$ in (59) is mismatched with the actual value because of the estimation error of the unknown parameters λ and b , now the design parameter M , is piecewise-constant with a single discontinuity at $t = t_M$, should satisfy

$$M > 0 \quad \& \quad M \neq \frac{-r(1)Y(0) - \hat{p}(1, 0)}{\text{sign}(\vartheta(y_1(0), 0))}, \quad t \in [0, t_M], \quad (90)$$

and

$$\left\{ \begin{array}{l} M > \frac{\sup_{t \geq t_M} \left| 2 \sum_{j=0}^{+\infty} e^{-\varepsilon(\frac{\pi}{2}+j\pi)^2 t} \hat{\theta}_j \right|}{1 - 2 \sum_{j=0}^{+\infty} e^{-\varepsilon(\frac{\pi}{2}+j\pi)^2 t_M} \frac{(-1)^j}{\frac{\pi}{2}+j\pi}}, t \geq t_M, \text{ if } t_M \geq t_1, \\ M > \max_{\lambda \leq \hat{\lambda}, 0 < b \leq \bar{b}} \frac{\sup_{t \geq t_M} \left| 2 \sum_{j=0}^{+\infty} e^{-\varepsilon(\frac{\pi}{2}+j\pi)^2 t} \hat{\theta}_j \right|}{1 - 2 \sum_{j=0}^{+\infty} e^{-\varepsilon(\frac{\pi}{2}+j\pi)^2 t_M} \frac{(-1)^j}{\frac{\pi}{2}+j\pi}}, t \geq t_M, \\ \text{if } t_M < t_1. \end{array} \right. \quad (91)$$

The equation (90) can ensure achieving fast identification of the unknown parameters at the first triggering time t_1 defined by (65), as will be shown in the next lemma.

Remark 1 We define $\dot{M}(t_M)$ as the right derivative, hence $\dot{M} = 0$ for all time. Alternatively, one may choose M sufficiently large in practice to avoid this discontinuity at $t = t_M$, at the expense of increased conservativeness.

Lemma 2 *The finite-time exact identification of the unknown parameters is achieved at the first update time instant t_1 , i.e.,*

$$\hat{\theta}(t) \equiv \theta, \quad \forall t \geq t_1. \quad (92)$$

Proof. We first prove that $u(0, t)$ is not identically zero for $t \in [0, t_1]$ by contradiction. Supposing that $u(0, t) \equiv 0$ for $t \in [0, t_1]$, together with (2) and (3), we have that $u(x, t) \equiv 0$ for all $x \in [0, 1]$ and $t \in [0, t_1]$, which implies that $u(1, t) = U_a(t) \equiv 0$ for $t \in [0, t_1]$. Recalling (90), (93), (37), we have that $U_a(0) \neq 0$: contradiction. Therefore, we have that $u(0, t)$ is not identically zero for $t \in [0, t_1]$. It means that that exists \bar{n} such that $Q_{\bar{n}, 1}(0, t_1) \neq 0$, and $Q_2(0, t_1) \neq 0$ according to (73), (71), (79), (80). It implies that $G_{\bar{n}}(0, t_1)$ is invertible recalling (76). Therefore, the output of (81) at t_1 , i.e., $\hat{\theta}(t_1)$, is indeed the true value θ considering (75). According to (64), (81), (75), We know that $\hat{\lambda}(t_{i+1})$ is equal to either λ or $\hat{\lambda}(t_i)$, and also $\hat{b}(t_{i+1})$ is equal to either b or $\hat{b}(t_i)$. We obtain from $\hat{\theta}(t_1) = \theta$ that $\hat{\theta}(t) = \theta$ for $t \in [t_1, \infty)$, considering (65) that implies $\lim_{i \rightarrow \infty} (t_i) \rightarrow \infty$. More detailed proof of the exact identification of the unknown parameter in the parabolic PDE-ODE system by BaLSI can be seen in [40]. \square

Finally, the safe adaptive controller $U_a(t)$ is obtained as

$$U_a(t) = \int_0^1 \hat{k}(1, y) u(y, t) dy + r(1) Y(t) + \delta(t) + \hat{p}(1, t), \quad (93)$$

where $\hat{k}(1, y)$, $\hat{p}(1, t)$ are obtained by submitting the estimates $\hat{\lambda}, \hat{b}$ into the $k(1, y)$, $p(1, t)$ defined in (A1), (A9), and where $\delta(t)$ is given by (37) with M satisfying (90), (91).

4.3 Results of safe adaptive control

Theorem 2 *For all initial data $u[0] \in L^2(0, 1)$, $Y(0) \in \mathbb{R}^n$, with the design parameters κ_i , $i = 1, 2, \dots$ satisfying (38)*

and $\kappa_n \leq c$, the closed-loop system including the plant (1)–(4) with the safe adaptive controller (93) has the following properties.

(1) *There exist unique mappings $u \in C^0(\mathbb{R}_+; L^2(0, 1)) \cap C^1(J \times [0, 1])$ with $u[t] \in C^2([0, 1])$, $Y \in C^0(\mathbb{R}_+; \mathbb{R}^n)$, where $J = \mathbb{R}_+ \setminus \{t_1\}$.*

(2) *All plant states are convergent to zero, i.e.,*

$$\lim_{t \rightarrow \infty} (\|u_x(\cdot, t)\|^2 + \|u(\cdot, t)\|^2 + |Y(t)|^2) = 0.$$

(3) *Safety is ensured in the sense that if $h(y_1(0), 0) > 0$, then $h(y_1(t), t) \geq 0$ for all $t \geq 0$; if $h(y_1(0), 0) \leq 0$, then there exists a finite time t_a ($t_a > t_1$) such that $h(y_1(t), t) \geq 0$ for all $t \geq t_a$, where t_a ($t_a > t_1$) can be assigned by users.*

Proof. (1) The property is straightforward to obtain following the proof of Corollary 1 in [40].

(2) According to the Lemma 2, we directly have that the parameter estimation error $\hat{\theta} = 0$, $\forall t \geq t_1$. Considering the Lyapunov function (46) for $t \in [0, t_1]$ and $t \in [t_1, \infty]$, respectively, choosing the analysis parameter a_1 and a_2 as (49) and (50), where the upper bound \bar{b} is used to replace the unknown b in (49) and (50). i.e., $a_1 > \max \left\{ \frac{3|P\bar{B}|^2 \bar{\delta}^2}{c\lambda_{\min}(\bar{Q})} - \frac{\varepsilon}{c}, 0 \right\}$ and $a_2 > \frac{3|P\bar{B}|^2 \bar{\delta}^2}{c\lambda_{\min}(\bar{Q})}$ with $\bar{B} = [0, 0, \dots, \bar{b}]^T$, following the proof below (51) in the proof of property 1 in Theorem 1, together with the fact that $V(t)$ (46) is continuous at $t = t_1$, which can be known from the property 1, we thus obtain the property 2 in this theorem.

(3) Similarly, like the proof of property 2 in Theorem 1, together with M satisfying (90) and (91), we have $h_1(z_1(t), t) > 0$ for all $t \geq 0$. Through the same process as the safety analysis in the two cases $h(y_1(0), 0) > 0$, $h(y_1(0), 0) \leq 0$ at the end of the proof of Theorem 1, property 3 is thus obtained.

The proof of this theorem is complete. \square

4.4 Simulation

The considered simulation model is (1)–(4) with the parameters $A = [a_{1,1}, 1; a_{2,1}, a_{2,2}] = [0, 1; 2, -1]$, $B = [0, b]^T = [0, 5]^T$, $\varepsilon = 1$, $\lambda = 10$. The known bounds of the unknown parameters λ , b are set as $\underline{\lambda} = 8$, $\bar{\lambda} = 12$, $\underline{b} = 3$, $\bar{b} = 7$. The simulation is conducted based on the finite difference method with a time step of 0.001 and a space step of 0.05. Some tips on the implementation of the parameter identifier (81) can be found in [40]. We conduct the simulation in the following two cases, each with a different safe barrier function.

Case 1: Safe condition $h(y_1(t), t)$ is defined as $h(y_1(t), t) = y_1(t)$. It means that $\vartheta = 1$. For $\sigma(t)$ in (18), we choose

$t_a = 1$ and $\beta = 1$. The initial values are defined as $y_2(0) = 0$, $u(x, 0) = x^2 \sin(4\pi x)$, $\hat{\lambda}_1(0) = 8$, $\hat{b}_1(0) = 7$, and $y_1(0)$ is defined as two subcases:

- $y_1(0) = 10$ for the initially safe subcase;
- $y_1(0) = -10$ for the initially unsafe subcase.

Based on the simulation model given above, we construct the safe adaptive controller $U_a(t)$ by choosing the design parameters as $\kappa_1 = 23$, $\kappa_2 = 3$, $M = 3000$. The arbitrary positive design parameters are set as $T = 0.5$, $\bar{n} = 1$, $\tilde{N} = 12$.

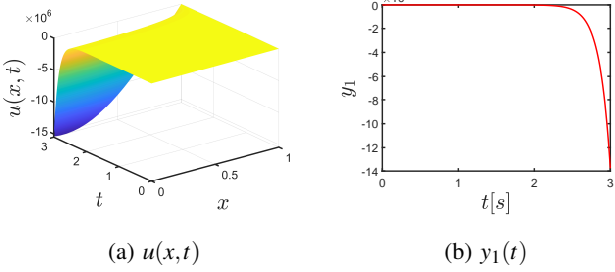


Fig. 1. Results of $u(x, t)$ and $y_1(t)$ in open-loop system

The simulation results of $u(x, t)$ and $y_1(t)$ in the open-loop system are presented in Fig 1a and 1b, which imply that the simulation model is open-loop unstable. The simulation results of the closed-loop system, under the nominal safe control and safe adaptive control, respectively, are given below.

(i) (initially safe $y_1(0) = 10$): The result of the output state $y_1(t)$ and the other state $y_2(t)$ in the ODE are shown in Figs 2 and 3, where the red solid line denotes the result with the safe adaptive controller U_a , while the blue solid line denotes the result with the nominal safe control U . We can see that both the safe adaptive controller and the nominal safe controller can not only ensure that the output y_1 converges to zero, but also keep $y_1(t)$ within the safe region throughout the entire process. The parameter estimates converge to the true values in the first triggering time, as shown in Fig 4, where the tiny difference between the final estimate $\hat{\lambda}$ and its true value comes from the approximation error of integration as explained in [42]. The results of $u(x, t)$ under the safe adaptive controller and nominal safe controller are shown in Figs 5a and 5b, respectively. It is observed that the system state $u(x, t)$ exhibits a noticeable jump at the first triggering time. This occurs because, at this triggering instant, the estimated parameters are updated, from the initial estimates to the true values, which causes the control input $U(t)$, in particular the term involving $p(1, t)$, to change abruptly. Nevertheless, after this, $u(x, t)$ rapidly converges to zero.

(ii) (initially unsafe $y_1(0) = -10$): In this subcase, the initial conditions are the same as in subcase i, except for $y_1(0)$, which is unsafe now. Under both nominal safe and safe adaptive controllers, all system states converge to zero fast. The true values of unknown parameters are also identified at the first triggering instant in the adaptive safe controller. These

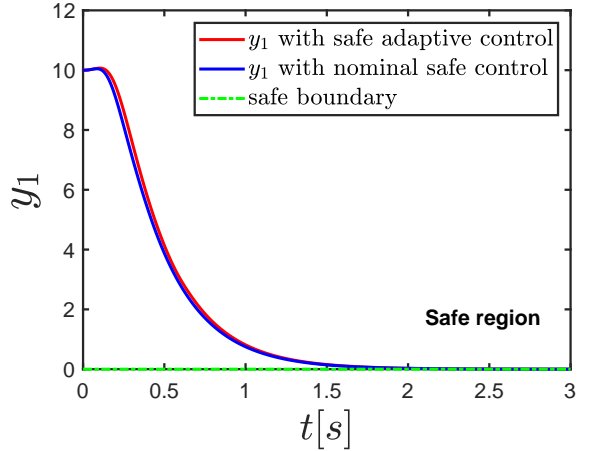


Fig. 2. The trajectory of $y_1(t)$ when the initial condition is safe

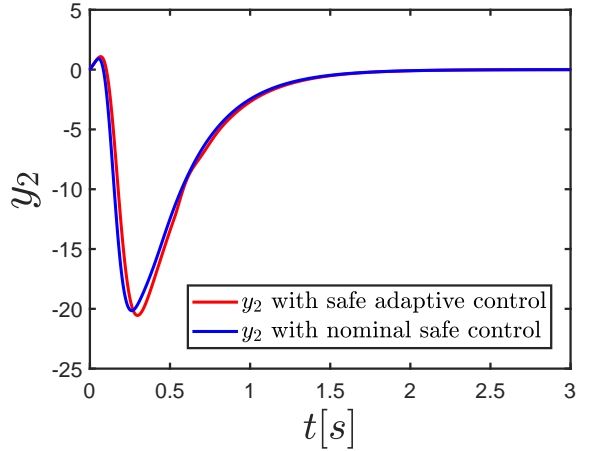


Fig. 3. The trajectory of $y_2(t)$ when the initial condition is safe

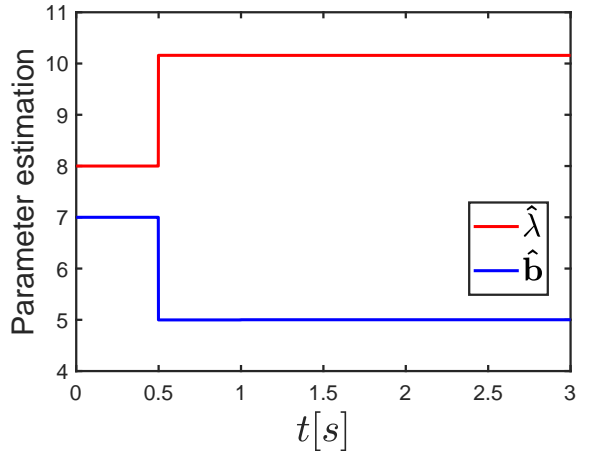
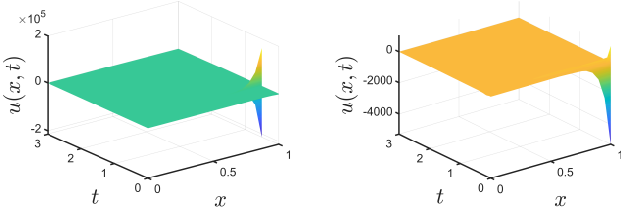


Fig. 4. Estimation of parameters when the initial condition is safe



(a) $u(x, t)$ with safe adaptive controller (b) $u(x, t)$ with nominal safe controller

Fig. 5. Results of $u(x, t)$ when the initial condition is safe

results are similar to Figs 2–5, which are not represented here to avoid repetition. The trajectory of the output state $y_1(t)$ is shown in Fig. 6, from which we can see that both the safe adaptive controller and the nominal safe controller can not only ensure that the output y_1 converges to zero, but also guide it back to the safe region (i.e., $y_1(t) \geq 0$), from the unsafe initial position $y_1(0) = -10$, in about 0.6 seconds (within the recovery time $t_a = 1\text{s}$), and then keep it in the safe region all the time.

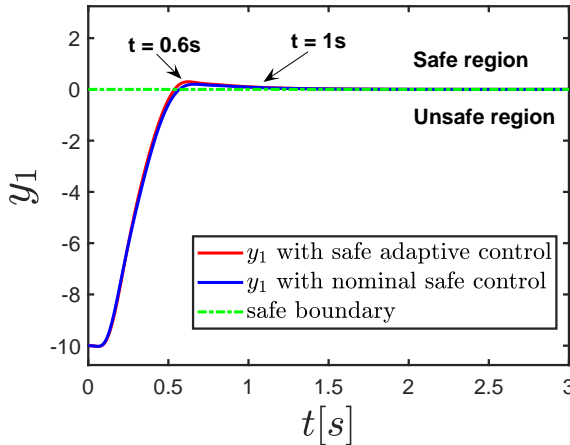


Fig. 6. The trajectory of $y_1(t)$ when the initial condition is unsafe

Case 2: The safe condition $h(y_1(t), t)$ is defined as $h(y_1(t), t) = ae^{-dt} - y_1(t)$. This implies that $\vartheta = -1$ and the safe region is $y_1(t) \leq ae^{-dt}$. The parameters are chosen as $a = 14$ and $d = 3$. Here, we select $\beta = 4$ and $M = 8000$. Two subcases for the initial condition $y_1(0)$ are considered:

- $y_1(0) = 10$ for the initially safe subcase;
- $y_1(0) = 18$ for the initially unsafe subcase.

Other conditions remain identical to Case 1. To avoid repetition, we only present the trajectory of the output state $y_1(t)$ in Fig. 7, since other results are similar to those in Case 1. Fig. 7 shows that both the safe adaptive controller and the nominal safe controller ensure that the output y_1 converges to zero. Moreover, when the initial value of y_1 locates at the unsafe region, i.e., $y_1(0) = 18 > a$, the proposed controller will guide it back to the safe region, i.e.,

$y_1(t) \leq ae^{-dt}$, within approximately 0.5 seconds (which is less than the prescribed safety recovery time $t_a = 1\text{s}$), and keep it within the safe region thereafter; when y_1 is initially safe, i.e., $y_1(0) = 10 < a$, the safety $y_1(t) \leq ae^{-dt}$ will be guaranteed all the time.

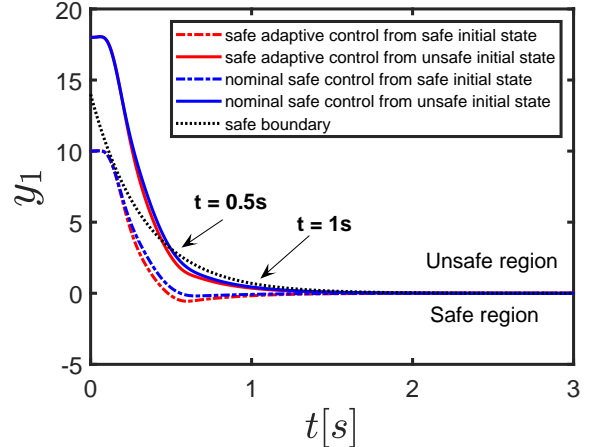


Fig. 7. The trajectory of $y_1(t)$

5 Conclusion and Future Work

This paper presents a safe adaptive control strategy for a class of parabolic PDE-ODE cascade systems subject to parameter uncertainties in both PDE and ODE subsystems. Under the proposed safe adaptive controller, the system output is guaranteed to remain safe at all times if the initial state is safe. Otherwise, the controller will regulate the system output into the safe region within a user-prescribed time. Furthermore, all system states are ensured to converge to zero. The effectiveness of the proposed control scheme is validated through numerical simulations.

In our future work, a practical physical application will be considered, incorporating the observer designs for system states and external disturbances.

Appendix

A Solution to (25)–(27)

According to [18], the solution to (25)–(27) is given by

$$k(x, y) = \sum_{n=0}^{\infty} \Delta G^n(\xi, \eta), \quad (\text{A1})$$

where

$$\xi = x + y, \quad (\text{A2})$$

$$\eta = x - y, \quad (\text{A3})$$

$$\begin{aligned} G(\xi, \eta) &= \frac{-(\lambda + c)}{4\epsilon}(\xi + \eta) + \int_0^\eta r(m)dm \frac{B}{\epsilon} \\ &+ \frac{\lambda + c}{2\epsilon} \int_0^\eta \left[\int_0^m G(m, \tau)d\tau \right] dm \\ &+ \frac{\lambda + c}{4\epsilon} \int_\eta^\xi \left[\int_0^\eta G(m, \tau)d\tau \right] dm, \end{aligned} \quad (\text{A4})$$

$$G^0(\xi, \eta) = 0, \quad (\text{A5})$$

$$\begin{aligned} G^{n+1}(\xi, \eta) &= \frac{-(\lambda + c)}{4\epsilon}(\xi + \eta) + \int_0^\eta r(m)dm \cdot \frac{B}{\epsilon} \\ &+ \frac{\lambda + c}{2\epsilon} \int_0^\eta \left[\int_0^m G^n(m, \tau)d\tau \right] dm \\ &+ \frac{\lambda + c}{4\epsilon} \int_\eta^\xi \left[\int_0^\eta G^n(m, \tau)d\tau \right] dm, \end{aligned} \quad (\text{A6})$$

$$\Delta G^n(\xi, \eta) = G^{n+1}(\xi, \eta) - G^n(\xi, \eta), \quad (\text{A7})$$

and the solution of (28), (29) is given by

$$r(x) = \begin{pmatrix} -K^T & 0 \end{pmatrix} e^{Dx} \begin{pmatrix} I \\ 0 \end{pmatrix}, D = \begin{pmatrix} 0 & \frac{A+cl}{\epsilon} \\ I & 0 \end{pmatrix}, \quad (\text{A8})$$

where I is the identity matrix. The solution of (30), (31) can be obtained by Taylor series as

$$\begin{aligned} p(x, t) &= p(0, t) + p_x(0, t)x + p_x^{(2)}(0, t) \frac{x^2}{2!} \\ &+ \cdots + p_x^{(m)}(0, t) \frac{x^m}{m!} + \cdots \end{aligned} \quad (\text{A9})$$

We can obtain the value of $p_x^{(m)}(0, t)$ for $m = 2, 3, \dots$ from (30) and its derivatives with respect to x , together with inserting $x = 0$ and recalling (31).

B Solving $w(x, t)$ in (33)–(35)

The detailed process for solving $w(x, t)$ is shown as follows. Considering (41), (33)–(35), we have

$$v_t(x, t) = \epsilon v_{xx}(x, t) - cv(x, t) - c\delta(t) - \dot{\delta}(t), \quad (\text{B1})$$

$$v_x(0, t) = 0, \quad (\text{B2})$$

$$v(1, t) = 0. \quad (\text{B3})$$

Noticing that $c\delta + \dot{\delta}$ in (B1) is in fact zero, because $\delta(t) = \text{sign}(\vartheta)M e^{-ct}$. We nevertheless keep it in the derivation and solve $w(x, t)$ in this general form to avoid repetitiveness, because this will be reused when solving $w(x, t)$ in the subsequent safe adaptive controller design.

By eigenfunction expansion, we can express $v(x, t)$ and $c\delta(t) + \dot{\delta}(t)$ as

$$v(x, t) = \sum_{j=0}^{\infty} v_j(t) \cos\left(\frac{\pi}{2} + j\pi\right)x, \quad (\text{B4})$$

$$c\delta(t) + \dot{\delta}(t) = \sum_{j=0}^{\infty} f_j(t) \cos\left(\frac{\pi}{2} + j\pi\right)x, \quad (\text{B5})$$

where

$$\begin{aligned} f_j(t) &= 2 \int_0^1 (c\delta(t) + \dot{\delta}(t)) \cos\left(\frac{\pi}{2} + j\pi\right)x dx \\ &= \frac{2(-1)^j}{\frac{\pi}{2} + j\pi} (c\delta(t) + \dot{\delta}(t)). \end{aligned} \quad (\text{B6})$$

Applying (B4), (B5), the left side of (B1) can then be expressed as

$$v_t(x, t) = \sum_{j=0}^{\infty} \dot{v}_j(t) \cos\left(\frac{\pi}{2} + j\pi\right)x, \quad (\text{B7})$$

and the right side of (B1) can be obtained as

$$\begin{aligned} \epsilon v_{xx}(x, t) - cv(x, t) - c\delta(t) - \dot{\delta}(t) \\ = \sum_{j=0}^{\infty} \left(-\epsilon \left(\frac{\pi}{2} + j\pi \right)^2 - c \right) v_j(t) \cos\left(\frac{\pi}{2} + j\pi\right)x \\ - \sum_{j=0}^{\infty} f_j(t) \cos\left(\frac{\pi}{2} + j\pi\right)x. \end{aligned} \quad (\text{B8})$$

Hence, we have

$$\dot{v}_j(t) = \left(-\epsilon \left(\frac{\pi}{2} + j\pi \right)^2 - c \right) v_j(t) - f_j(t), \quad (\text{B9})$$

for each $j = 0, 1, 2, \dots$, which is a linear ordinary differential equation, whose solution is

$$\begin{aligned} v_j(t) &= e^{(-\epsilon(\frac{\pi}{2} + j\pi)^2 - c)t} \left[\theta_j - \int_0^t e^{(\epsilon(\frac{\pi}{2} + j\pi)^2 + c)\tau} f_j(\tau) d\tau \right] \\ &= -\frac{2(-1)^j}{\frac{\pi}{2} + j\pi} \int_0^t e^{-(\epsilon(\frac{\pi}{2} + j\pi)^2 + c)(t-\tau)} (c\delta(\tau) + \dot{\delta}(\tau)) d\tau \\ &+ e^{-(\epsilon(\frac{\pi}{2} + j\pi)^2 + c)t} \theta_j, \end{aligned} \quad (\text{B10})$$

for $\theta_j = v_j(0)$ to be determined later. Thus, recalling (B4), we obtain

$$\begin{aligned} v(x, t) &= \sum_{j=0}^{\infty} \cos\left(\frac{\pi}{2} + j\pi\right)x \times \left[e^{-(\epsilon(\frac{\pi}{2} + j\pi)^2 + c)t} \theta_j \right. \\ &\quad \left. - \frac{2(-1)^j}{\frac{\pi}{2} + j\pi} \int_0^t e^{-(\epsilon(\frac{\pi}{2} + j\pi)^2 + c)(t-\tau)} (c\delta(\tau) + \dot{\delta}(\tau)) d\tau \right]. \end{aligned} \quad (\text{B11})$$

Considering $v(x, 0) = u(x, 0) - \delta(0)$, it is obtained from (B11) that

$$v(x, 0) = \sum_{j=0}^{\infty} \theta_j \cos\left(\frac{\pi}{2} + j\pi\right)x = w(x, 0) - \delta(0). \quad (\text{B12})$$

Clearly, θ_j here are the Fourier coefficients of $w(x, 0) - \delta(0)$, that is,

$$\theta_j = 2 \int_0^1 (w(x, 0) - \delta(0)) \cos\left(\frac{\pi}{2} + j\pi\right) x dx. \quad (\text{B13})$$

Finally, we obtain the solution of $w(x, t)$ as (57).

C Proof of (61)

We prove (61) by showing that the following equation

$$S(\tau) = \vartheta \left[\text{sign}(\vartheta) - 2 \text{sign}(\vartheta(y_1(0), 0)) \sum_{j=0}^{\infty} e^{-\varepsilon(\frac{\pi}{2} + j\pi)^2 \tau} \frac{(-1)^j}{\frac{\pi}{2} + j\pi} \right] \geq 0, \quad (\text{C1})$$

holds for all $\tau > 0$. We propose the following claim that will be used in proving (C1).

Claim 1 For all $x > 0$, we have

$$0 < \sum_{j=0}^{\infty} e^{-(2j+1)^2 x} \frac{(-1)^j}{2j+1} < \pi/4. \quad (\text{C2})$$

Proof. We now define a function $L(x)$ as

$$L(x) = \pi/4 - \sum_{j=0}^{\infty} \frac{(-1)^j}{2j+1} e^{-(2j+1)^2 x}, \quad (\text{C3})$$

where

$$L(0) = \pi/4 - \sum_{j=0}^{\infty} \frac{(-1)^j}{2j+1} = \pi/4 - \arctan(1) = 0. \quad (\text{C4})$$

Next, we will prove that $0 < L(x) < \frac{\pi}{4}$ for all $x > 0$. First, we differentiate $L(x)$ with respect to x .

$$\dot{L}(x) = \sum_{j=0}^{\infty} (-1)^j (2j+1) e^{-(2j+1)^2 x}. \quad (\text{C5})$$

Then we introduce a type of Jacobi theta function $\vartheta_1(z, q)$, which is defined in [46, Ch.21] as follows:

$$\vartheta_1(z, q) = 2 \sum_{j=0}^{\infty} (-1)^j q^{(j+\frac{1}{2})^2} \sin((2j+1)z). \quad (\text{C6})$$

Differentiating (C6) with respect to z , we have

$$\frac{\partial \vartheta_1(z, q)}{\partial z} = 2 \sum_{j=0}^{\infty} (-1)^j (2j+1) q^{(j+\frac{1}{2})^2} \cos((2j+1)z). \quad (\text{C7})$$

Setting $z = 0$ and $q = e^{-4x}$, we obtain

$$\frac{\partial \vartheta_1(0, e^{-4x})}{\partial z} = 2 \sum_{j=0}^{\infty} (-1)^j (2j+1) e^{-(2j+1)^2 x}. \quad (\text{C8})$$

Comparing with (C5), we know $\dot{L}(x) = \frac{1}{2} \frac{\partial \vartheta_1(0, e^{-4x})}{\partial z}$. According to [46, Ch.21], we know that

$$\frac{\partial \vartheta_1(0, e^{-4x})}{\partial z} = 2e^{-x} \prod_{j=1}^{\infty} (1 - e^{-8jx}) \prod_{j=1}^{\infty} (1 - e^{-8jx})^2. \quad (\text{C9})$$

Since $x > 0$, we can easily obtain that $\frac{\partial \vartheta_1(0, e^{-4x})}{\partial z} > 0$. Therefore, we have $\dot{L}(x) > 0$ for all $x > 0$. Noticing that $L(0) = 0$ and $\lim_{x \rightarrow +\infty} L(x) = \frac{\pi}{4}$, we can conclude that $0 < L(x) < \frac{\pi}{4}$ for all $x > 0$. The proof of the claim is complete. \square

Now, we continue to prove (C1). We consider two cases:

(1) $\vartheta(y_1(0), 0) > 0$. In this case, we have

$$S(\tau) = \vartheta \left[\text{sign}(\vartheta) - 2 \sum_{j=0}^{\infty} e^{-\varepsilon(\frac{\pi}{2} + j\pi)^2 \tau} \frac{(-1)^j}{\frac{\pi}{2} + j\pi} \right]. \quad (\text{C10})$$

According to Claim 1, we have

$$\begin{aligned} S(\tau) &= \vartheta \left[1 - \frac{4}{\pi} \sum_{j=0}^{\infty} e^{-\varepsilon(\frac{\pi}{2} + j\pi)^2 \tau} \frac{(-1)^j}{2j+1} \right] \\ &= \frac{4\vartheta}{\pi} \left[\frac{\pi}{4} - \sum_{j=0}^{\infty} e^{-\varepsilon \frac{\pi^2}{4} \tau (1+2j)^2} \frac{(-1)^j}{2j+1} \right] \\ &> 0, \end{aligned} \quad (\text{C11})$$

for $\vartheta > 0$. If $\vartheta < 0$, we have

$$\begin{aligned} S(\tau) &= \vartheta \left[-1 - \frac{4}{\pi} \sum_{j=0}^{\infty} e^{-\varepsilon(\frac{\pi}{2} + j\pi)^2 \tau} \frac{(-1)^j}{2j+1} \right] \\ &= -\frac{4\vartheta}{\pi} \left[\frac{\pi}{4} + \sum_{j=0}^{\infty} e^{-\varepsilon \frac{\pi^2}{4} \tau (1+2j)^2} \frac{(-1)^j}{2j+1} \right] \\ &> 0, \end{aligned} \quad (\text{C12})$$

because of $\sum_{j=0}^{\infty} e^{-\varepsilon \frac{\pi^2}{4} \tau (1+2j)^2} \frac{(-1)^j}{2j+1} > 0$ according to Claim 1.

(2) $\vartheta(y_1(0), 0) < 0$. In this case, we have

$$S(\tau) = \vartheta \left[\text{sign}(\vartheta) + 2 \sum_{j=0}^{\infty} e^{-\varepsilon(\frac{\pi}{2} + j\pi)^2 \tau} \frac{(-1)^j}{\frac{\pi}{2} + j\pi} \right]. \quad (\text{C13})$$

Similarly like the above case 1, we can directly obtain that $S(\tau) \geq 0$ for all $\tau > 0$.

Inequality (C1) is thus obtained.

D Proof of $h_n(\underline{z}_n(t), t) > 0$ for all $t \geq 0$

Recalling the expression of $h_n(\underline{z}_n(t), t)$ in (56), we can obtain that

$$\begin{aligned} e^{\kappa_n \tau} \vartheta w(0, \tau) &= e^{(\kappa_n - c)\tau} \vartheta \left[\text{sign}(\vartheta) M \right. \\ &\quad - 2 \text{sign}(\vartheta(y_1(0), 0)) M \sum_{j=0}^{+\infty} e^{-\varepsilon(\frac{\pi}{2}+j\pi)^2 \tau} \frac{(-1)^j}{\frac{\pi}{2}+j\pi} \\ &\quad \left. + 2 \sum_{j=0}^{+\infty} e^{-\varepsilon(\frac{\pi}{2}+j\pi)^2 \tau} \dot{\theta}_j \right], \end{aligned} \quad (\text{D1})$$

for $\vartheta > 0$, we rewrite the above expression as

$$\begin{aligned} e^{\kappa_n \tau} \vartheta w(0, \tau) &= e^{(\kappa_n - c)\tau} \vartheta \left[M \right. \\ &\quad - 2 \text{sign}(\vartheta(y_1(0), 0)) M \sum_{j=0}^{+\infty} e^{-\varepsilon(\frac{\pi}{2}+j\pi)^2 \tau} \frac{(-1)^j}{\frac{\pi}{2}+j\pi} \\ &\quad \left. + 2 \sum_{j=0}^{+\infty} e^{-\varepsilon(\frac{\pi}{2}+j\pi)^2 \tau} \dot{\theta}_j \right]. \end{aligned} \quad (\text{D2})$$

Considering (62) and Claim 1, we know

$$M > \frac{\sup_{t \geq t_M} \left| 2 \sum_{j=0}^{+\infty} e^{-\varepsilon(\frac{\pi}{2}+j\pi)^2 t} \dot{\theta}_j \right|}{1 + 2 \sum_{j=0}^{+\infty} e^{-\varepsilon(\frac{\pi}{2}+j\pi)^2 t_M} \frac{(-1)^j}{\frac{\pi}{2}+j\pi}}. \quad (\text{D3})$$

So we have

$$M > \frac{\sup_{t \geq t_M} \left| 2 \sum_{j=0}^{+\infty} e^{-\varepsilon(\frac{\pi}{2}+j\pi)^2 t} \dot{\theta}_j \right|}{1 - 2 \text{sign}(\vartheta(y_1(0), 0)) \sum_{j=0}^{+\infty} e^{-\varepsilon(\frac{\pi}{2}+j\pi)^2 t_M} \frac{(-1)^j}{\frac{\pi}{2}+j\pi}}. \quad (\text{D4})$$

Inserting (D4) into (D1), we obtain that $e^{\kappa_n \tau} \vartheta w(0, \tau) > 0$ for all $t \geq t_M$.

Similarly, for $\vartheta < 0$, we rewrite the expression (D1) as

$$\begin{aligned} e^{\kappa_n \tau} \vartheta w(0, \tau) &= e^{(\kappa_n - c)\tau} (-\vartheta) \left[M \right. \\ &\quad + 2 \text{sign}(\vartheta(y_1(0), 0)) M \sum_{j=0}^{+\infty} e^{-\varepsilon(\frac{\pi}{2}+j\pi)^2 \tau} \frac{(-1)^j}{\frac{\pi}{2}+j\pi} \\ &\quad \left. - 2 \sum_{j=0}^{+\infty} e^{-\varepsilon(\frac{\pi}{2}+j\pi)^2 \tau} \dot{\theta}_j \right]. \end{aligned} \quad (\text{D5})$$

Considering (62) and Claim 1, we have

$$M > \frac{\sup_{t \geq t_M} \left| 2 \sum_{j=0}^{+\infty} e^{-\varepsilon(\frac{\pi}{2}+j\pi)^2 t} \dot{\theta}_j \right|}{1 + 2 \text{sign}(\vartheta(y_1(0), 0)) \sum_{j=0}^{+\infty} e^{-\varepsilon(\frac{\pi}{2}+j\pi)^2 t_M} \frac{(-1)^j}{\frac{\pi}{2}+j\pi}}. \quad (\text{D6})$$

Inserting (D6) into (D5), we have $e^{\kappa_n \tau} \vartheta w(0, \tau) > 0$ for all $t \geq t_M$.

Overall, we get $e^{\kappa_n \tau} \vartheta w(0, \tau) > 0$ for all $t \geq t_M$. Then considering (56) and the fact that $h_n(\underline{z}_n(0), 0) > 0$ and $h_n(\underline{z}_n(t), t) > 0$ for all $t \in [0, t_M]$, we can obtain that $h_n(\underline{z}_n(t), t) > 0$ for all $t \geq 0$.

E Proof of the convergence of the series in (62)

We prove that the following series

$$\sum_{j=0}^{+\infty} e^{-\varepsilon(\frac{\pi}{2}+j\pi)^2 t} \dot{\theta}_j, \quad (\text{E1})$$

$$\sum_{j=0}^{+\infty} e^{-\varepsilon(\frac{\pi}{2}+j\pi)^2 t} \frac{(-1)^j}{\frac{\pi}{2}+j\pi} \quad (\text{E2})$$

converge for all $t > 0$.

Proof. Considering (59), the series of (E1), and applying Cauchy-Schwarz Inequality, we have

$$\begin{aligned} &\sum_{j=0}^{+\infty} e^{-\varepsilon(\frac{\pi}{2}+j\pi)^2 t} |\dot{\theta}_j| \\ &\leq \sum_{j=0}^{+\infty} e^{-\varepsilon(\frac{\pi}{2}+j\pi)^2 t} \sqrt{\frac{1}{2} \int_0^1 w(x, 0)^2 dx} \\ &\leq \sqrt{\frac{1}{2} \int_0^1 w(x, 0)^2 dx} \sum_{j=0}^{+\infty} e^{-\varepsilon(\frac{\pi}{2}+j\pi)^2 t}, \end{aligned} \quad (\text{E3})$$

for any $t > 0$. Since $\sum_{j=0}^{+\infty} e^{-\varepsilon(\frac{\pi}{2}+j\pi)^2 t}$ is a convergent series for all $t > 0$, we can conclude that the series in (E1) is absolutely convergent for all $t > 0$.

Next, we consider the alternating series in (E2). For any $t > 0$, we have that $e^{-\varepsilon(\frac{\pi}{2}+j\pi)^2 t} \frac{1}{\frac{\pi}{2}+j\pi}$ is monotonically decreasing as j increases and approaches zero as $j \rightarrow +\infty$. Therefore, according to Leibniz criterion for alternating series, we can conclude that the series in (E2) is absolutely convergent for all $t > 0$. The proof is complete. \square

References

[1] I. Abel, D. Steeves, M. Krstić, and M. Janković. Prescribed-time safety design for strict-feedback nonlinear systems. *IEEE Transactions on Automatic Control*, 69(3):1464–1479, 2023.

[2] T. Ahmed-Ali, F. Giri, M. Krstić, L. Burlion, and F. Lamnabhi-Lagarrigue. Adaptive boundary observer for parabolic PDEs subject to domain and boundary parameter uncertainties. *Automatica*, 72:115–122, 2016.

[3] T. Ahmed-Ali, F. Giri, M. Krstić, F. Lamnabhi-Lagarrigue, and L. Burlion. Adaptive observer for a class of parabolic PDEs. *IEEE Transactions on Automatic Control*, 61(10):3083–3090, 2015.

[4] A. D. Ames, X. Xu, J. W. Grizzle, and P. Tabuada. Control barrier function based quadratic programs for safety critical systems. *IEEE Transactions on Automatic Control*, 62(8):3861–3876, 2016.

[5] A. Baccoli, A. Pisano, and Y. Orlov. Boundary control of coupled reaction–diffusion processes with constant parameters. *Automatica*, 54:80–90, 2015.

[6] J. Deutscher. Backstepping design of robust output feedback regulators for boundary controlled parabolic PDEs. *IEEE Transactions on Automatic Control*, 61(8):2288–2294, 2015.

[7] I. Karafyllis, M. Kontorinaki, and M. Krstić. Adaptive control by regulation-triggered batch least squares. *IEEE Transactions on Automatic Control*, 65(7):2842–2855, 2019.

[8] I. Karafyllis and M. Krstić. Adaptive certainty-equivalence control with regulation-triggered finite-time least-squares identification. *IEEE Transactions on Automatic Control*, 63(10):3261–3275, 2018.

[9] I. Karafyllis, M. Krstić, and K. Chrysafi. Adaptive boundary control of constant-parameter reaction–diffusion PDEs using regulation-triggered finite-time identification. *Automatica*, 103:166–179, 2019.

[10] S. Koga, L. Camacho-Solorio, and M. Krstić. State estimation for lithium-ion batteries with phase transition materials via boundary observers. *Journal of Dynamic Systems, Measurement, and Control*, 143(4):041004, 2021.

[11] S. Koga, M. Diagne, and M. Krstić. Control and state estimation of the one-phase stefan problem via backstepping design. *IEEE Transactions on Automatic Control*, 64(2):510–525, 2018.

[12] S. Koga and M. Krstić. Safe PDE backstepping QP control with high relative degree CBFs: Stefan model with actuator dynamics. *IEEE Transactions on Automatic Control*, 68(12):7195–7208, 2023.

[13] M. Krstić. Compensating actuator and sensor dynamics governed by diffusion PDEs. *Systems & Control Letters*, 58(5):372–377, 2009.

[14] M. Krstić and M. Bement. Nonovershooting control of strict-feedback nonlinear systems. *IEEE Transactions on Automatic Control*, 51(12):1938–1943, 2006.

[15] M. Krstić and P. V. Kokotović. Control lyapunov functions for adaptive nonlinear stabilization. *Systems & Control Letters*, 26(1):17–23, 1995.

[16] M. Krstić and A. Smyshlyaev. Adaptive boundary control for unstable parabolic PDEs—Part I: Lyapunov design. *IEEE Transactions on Automatic Control*, 53(7):1575–1591, 2008.

[17] M. Krstić and A. Smyshlyaev. *Boundary control of PDEs: A course on backstepping designs*. SIAM, 2008.

[18] J. Li and Y. Liu. Adaptive control of uncertain coupled reaction–diffusion dynamics with equidiffusivity in the actuation path of an ODE system. *IEEE Transactions on Automatic Control*, 66(2):802–809, 2020.

[19] J. Li, Z. Wu, and Y. Liu. Condition-based adaptive scheme for the stabilization of an uncertain reaction–diffusion equation with nonlinear dynamic boundary. *IEEE Transactions on Automatic Control*, 69(12):8758–8765, 2024.

[20] W. Li and M. Krstić. Mean-nonovershooting control of stochastic nonlinear systems. *IEEE Transactions on Automatic Control*, 66(12):5756–5771, 2020.

[21] W. J. Liu. Boundary feedback stabilization of an unstable heat equation. *SIAM journal on control and optimization*, 42(3):1033–1043, 2003.

[22] W. J. Liu and M. Krstić. Backstepping boundary control of burgers’ equation with actuator dynamics. *Systems & Control Letters*, 41(4):291–303, 2000.

[23] B. T. Lopez and J. J. Slotine. Unmatched control barrier functions: Certainty equivalence adaptive safety. *arXiv preprint arXiv:2207.13873*, 2022.

[24] B. T. Lopez, J. J. E. Slotine, and J. P. How. Robust adaptive control barrier functions: An adaptive and data-driven approach to safety. *IEEE Control Systems Letters*, 5(3):1031–1036, 2020.

[25] M. Maghenem, A. J. Taylor, A. D. Ames, and R. G. Sanfelice. Adaptive safety using control barrier functions and hybrid adaptation. In *2021 American Control Conference (ACC)*, pages 2418–2423. IEEE, 2021.

[26] T. Meurer and A. Kugi. Tracking control for boundary controlled parabolic PDEs with varying parameters: Combining backstepping and differential flatness. *Automatica*, 45(5):1182–1194, 2009.

[27] Q. Nguyen and K. Sreenath. Exponential control barrier functions for enforcing high relative-degree safety-critical constraints. In *2016 American Control Conference (ACC)*, pages 322–328. IEEE, 2016.

[28] Y. Orlov, A. Pisano, A. Pilloni, and E. Usai. Output feedback stabilization of coupled reaction-diffusion processes with constant parameters. *SIAM Journal on Control and Optimization*, 55(6):4112–4155, 2017.

[29] B. Petrus, J. Bentsman, and B. G. Thomas. Enthalpy-based feedback control algorithms for the stefan problem. In *2012 IEEE 51st IEEE conference on decision and control (cdc)*, pages 7037–7042. IEEE, 2012.

[30] A. Pisano and Y. Orlov. Boundary second-order sliding-mode control of an uncertain heat process with unbounded matched perturbation. *Automatica*, 48(8):1768–1775, 2012.

[31] A. Smyshlyaev and M. Krstić. Adaptive boundary control for unstable parabolic PDEs—Part III: Output feedback examples with swapping identifiers. *Automatica*, 43(9):1557–1564, 2007.

[32] A. Smyshlyaev and M. Krstić. *Adaptive control of parabolic PDEs*. Princeton University Press, 2010.

[33] G. A. Susto and M. Krstić. Control of PDE–ODE cascades with neumann interconnections. *Journal of the Franklin Institute*, 347(1):284–314, 2010.

[34] S. X. Tang, L. Camacho-Solorio, Y. Wang, and M. Krstić. State-of-charge estimation from a thermal-electrochemical model of lithium-ion batteries. *Automatica*, 83:206–219, 2017.

[35] S. X. Tang and C. K. Xie. State and output feedback boundary control for a coupled PDE–ODE system. *Systems & Control Letters*, 60(8):540–545, 2011.

[36] A. J. Taylor and A. D. Ames. Adaptive safety with control barrier functions. In *2020 American Control Conference (ACC)*, pages 1399–1405. IEEE, 2020.

[37] R. Vazquez and M. Krstić. Control of 1-D parabolic PDEs with volterra nonlinearities, Part I: Design. *Automatica*, 44(11):2778–2790, 2008.

[38] R. Vazquez and M. Krstić. Control of 1D parabolic PDEs with volterra nonlinearities, Part II: analysis. *Automatica*, 44(11):2791–2803, 2008.

[39] R. Vazquez and M. Krstić. Boundary control and estimation of reaction–diffusion equations on the sphere under revolution symmetry conditions. *International Journal of Control*, 92(1):2–11, 2019.

[40] J. Wang and M. Krstić. Event-triggered adaptive control of a parabolic PDE–ODE cascade with piecewise-constant inputs and identification. *IEEE Transactions on Automatic Control*, 68(9):5493–5508, 2022.

[41] J. Wang and M. Krstić. Regulation-triggered adaptive control of a hyperbolic PDE–ODE model with boundary interconnections. *International Journal of Adaptive Control and Signal Processing*, 35(8):1513–1543, 2021.

- [42] J. Wang and M. Krstić. Output-positive adaptive control of hyperbolic PDE–ODE cascades. *IEEE Transactions on Automatic Control*, 2025.
- [43] J. Wang and M. Krstić. Safe output regulation of coupled hyperbolic PDE–ODE systems, 2025.
- [44] S. Wang and M. Diagne. Adaptive boundary control of reaction–diffusion PDEs with unknown distributed delay and unknown parameters. *IMA Journal of Mathematical Control and Information*, 42(4):dnaf034, 2025.
- [45] S. Wang, M. Diagne, and M. Krstić. Deep learning of delay-compensated backstepping for reaction-diffusion PDEs. *IEEE Transactions on Automatic Control*, 2025.
- [46] E. T. Whittaker and G. N. Watson. *A course of modern analysis*. Cambridge University Press, 2020.
- [47] W. Xiao and C. Belta. Control barrier functions for systems with high relative degree. In *2019 IEEE 58th conference on decision and control (CDC)*, pages 474–479. IEEE, 2019.
- [48] W. Xiao and C. Belta. High-order control barrier functions. *IEEE Transactions on Automatic Control*, 67(7):3655–3662, 2021.
- [49] X. Xu, L. Liu, M. Krstić, and G. Feng. Stabilization of chains of linear parabolic PDE–ODE cascades. *Automatica*, 148:110763, 2023.